Accepted Manuscript

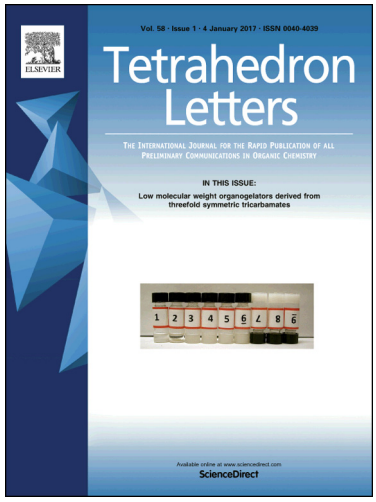

An efficient material via meta-position connection as thermally activated delayed fluorescence emitter for Organic Light-Emitting Diodes

Yuting Cui, Jianhui Liu

PII: S0040-4039(17)30304-0
DOI: http://dx.doi.org/10.1016/j.tetlet.2017.03.018
Reference: TETL 48719

To appear in: *Tetrahedron Letters*

Received Date: 12 January 2017
Revised Date: 2 March 2017
Accepted Date: 7 March 2017

Please cite this article as: Cui, Y., Liu, J., An efficient material via meta-position connection as thermally activated delayed fluorescence emitter for Organic Light-Emitting Diodes, *Tetrahedron Letters* (2017), doi: http://dx.doi.org/10.1016/j.tetlet.2017.03.018

An efficient material via meta-position connection as thermally activated delayed fluorescence emitter for Organic Light-Emitting Diodes

Yuting Cui[a], Jianhui Liu[a, b *]

[a]School of Petroleum and Chemical Engineering, Dalian University of Technology, Panjin Campus, Panjin, Liaoning Province 124221, PR China
[b]State Key Laboratory of Fine Chemicals, Dalian University of Technology, Dalian 116024, PR China

* Corresponding author.
E-mail address: liujh@dlut.edu.cn (J. Liu).
Tel: +86-138-98426106

Abstract

A novel compound was designed and synthesized by connecting a dicyanobenzene acceptor and two 9,9-dimethyl-9,10-dihydroacridine donors to the 1,3,5-position of a phenyl ring by *meta*-position connection. This compound, which is a novel emitter for OLED devices, exhibits preferable heat stability. Moreover, the energy gap between its singlet and triplet states is as small as 0.04 eV, resulting in this molecule possesses thermally activated delayed fluorescence. Therefore, the corresponding device showed efficient electroluminescent performances. The maximum external quantum efficiency, maximum current efficiency, maximum power efficiency and maximum luminance were 16.5%, 40.8 cd A^{-1}, 45.8 lm W^{-1} and 5120 cd m^{-2}, respectively. In addition, the $CIE_{x,y}$ only changed from (0.22, 0.38) to (0.22, 0.39) over the entire operating voltage range, which confirms that the device possesses highly stable chromaticity with respect to the current density. Based on these experimental results, *meta*-connected type structures may provide a new approach for developing high-performance TADF emitters for OLED applications.

Keywords: TADF, donor-acceptor structure, *meta*-position connection, OLED

Introduction

In the past two decades, organic light-emitting diodes (OLEDs) have attracted considerable attention due to their enormous potential for applications in both new generation full-color flat-panel displays and solid-state lighting sources.[1-3] As this new

technology rapidly evolves, the growth of organic emissive materials has also increased rapidly.[4-6] In particular, considerable successes have been reported for heavy metal complex phosphorescent emitters, which can comprehensively utilize both singlet (25%) and triplet (75%) excitons via spin orbit coupling between heavy metals and their ligands to achieve an internal quantum efficiency (IQE) of nearly 100%.[7, 8] However, rare metal elements, such as Ir, Pt, Ru, Os and Au, are indispensably included in most phosphorescent emitters.[9-11] Their high cost makes phosphorescent emitters unpopular for large-scale commercial production. Therefore, an increasing number of scientists have focused on pure organic thermally activated delayed fluorescence (TADF) emitters, which are the newest type of emitters.[6, 12] Due to non-radiative triplet excitons that can be thermally driven into a radiative singlet state, TADF emitters can theoretically approach an IQE of 100% without the use of noble metals.[13, 14] A small singlet-triplet energy gap (ΔE_{ST}) is essential to realizing TADF emission since the reverse intersystem crossing (RISC) process only occurs if the energy barrier between the singlet and triplet states can be overcome.[15, 16] To achieve a small ΔE_{ST}, TADF emitters should be designed with separated highest occupied molecular orbital (HOMO) and lowest unoccupied molecular orbital (LUMO). This separation could allow for the triplet energy of the molecules to be maintained in a high level to the largest extent.[17, 18] Therefore, charge-transfer type molecules with donor-acceptor structures might enable highly efficient TADF emitters.[19, 20]

Most of the previously reported TADF emitters include π-bridge units, such as a benzene ring, to connect their donor and acceptor moieties. In addition, substantial steric hindrance between the donor/acceptor and the π-bridge will result in large dihedral angles and separated HOMO and LUMO distributions. In general, donor and acceptor moieties are connected via the *para*-position of the phenyl linker to empirically achieve high photoluminescence quantum yields (PLQYs). For example, DMAC-DPS, which are constructed from diphenylsulfone and acridine, is a typical representative of this type of emitter.[21] However, the feasibility of achieving efficient TADF emitters by connecting donor and acceptor components through the *meta*-position has been neglected.[6, 22] Herein, a novel compound that was designed by connecting a dicyanobenzene acceptor and two 9,9-dimethyl-9,10-dihydroacridine donors at the 1, 3, 5-position of a benzene ring was prepared as an efficient TADF emitting molecule. The investigated emitter (DAB-DCNB) exhibited a small ΔE_{ST} of 0.04 eV and a short excited state lifetime of 7.1 μs. An emission peak at 497 nm and a satisfactorily PLQY were obtained. Therefore, a sky-blue TADF device with an EQE of 16.5% was demonstrated in this study. Furthermore, the reported EQE is one of the highest among devices using *meta*-connected type emitters.[23, 24]

Results and discussion

DAB-DCNB was expected to exhibit a small ΔE_{ST} by controlling the charge transfer (CT) and conjugation in an appropriate degree via connection at the *meta*-position. The adoption of a *meta*-type connection will weaken the inductive effect that originates from the electron withdrawing abilities of the acceptor unit, prevents reduction of the singlet energies and causes a blue-shifted emission.

Moreover, because the *meta*-linkage can decrease the conjugation length of the entire compound to a shorter extent than that in *para*-position compounds, it is beneficial to maintain the triplet states at a high energy level. Therefore, *meta*-connected type compounds can exhibit a small ΔE_{ST} and serve as TADF emitters. The suitable energy levels, good thermal stability and distinct photophysical properties make **DAB-DCNB** a good candidate for TADF OLEDs, and the pivotal electrochemical, photophysical and thermal properties are summarized in Table 1.

Table 1. Physical properties of **DAB-DCNB**

$\lambda_{max,Abs}$[a] [nm]	$\lambda_{max,PL}$[a] [nm]	$\lambda_{max,PL}$[b] [nm]	HOMO [eV]	LUMO[c] [eV]	E_g^{opt} [eV]	PLQY (neat film) [%]	PLQY (doped film) [%]	Calculated ΔE_{ST} [eV]	Experimental ΔE_{ST} [eV]	T_d [℃]
209	508	487	-5.07	-2.21	2.86	52	61	0.03 eV	0.04	383

[a] UV-vis absorption and PL peaks for neat thin film.

[b] PL peaks for doped thin film (10% emitter doped in mCP).

[c] Conclude from HOMO and ΔE_g^{opt} (ΔE_g^{opt} =1240/λ_{onset}, λ_{onset} is the onset wavelength of absorption spectra).

Figure 1 show the molecular model (Fig. 1a) as well as the HOMO and LUMO distributions from density functional theory (DFT) calculations using the B3LYP 6-31G (d) basis set as implemented in the Gaussian 09 program. The HOMO was evenly located on the two acridine moieties and slightly permeated into the central benzene ring of the relevant molecule, and the LUMO was primarily dispersed over the dicyanobenzene unit (Fig. 1b). These results can be attributed to large torsion angles between the donors/acceptor and the phenyl π-bridge due to the substantial steric hindrance that effectively separate the HOMO and LUMO of **DAB-DCNB**. Consistent with the original design intention of this emitter, a time-dependent density functional theory (TD-DFT) simulation predicted that the ΔE_{ST} of **DAB-DCNB** will be small as 0.03 eV, which is favorable to achieve TADF characteristics (Table 1). The synthetic route and structure of **DAB-DCNB** is shown in Scheme 1. First, compound **1** was synthesized according to previously reported procedures.[25] Then, precursor **2** was prepared via Suzuki cross-coupling reactions. Finally, the target product was obtained via a palladium-catalyzed reaction and purified by column chromatography followed by vacuum sublimation to afford the pure product in a 61% yield. ^{1}H and ^{13}C NMR (Figs. S1-S6, Supplementary Material), mass spectrometer and elemental analyses were employed to confirm the chemical structures of compound **1**, precursor **2** and the target compound.

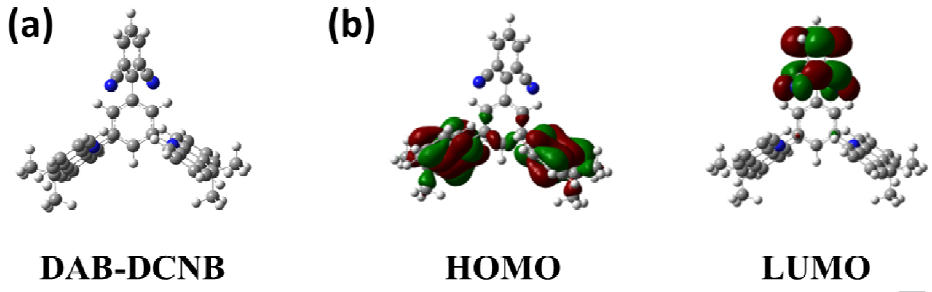

Figure 1. (a) Optimized molecular structure of **DAB-DCNB** and (b) HOMO and LUMO distributions from the DFT calculations with the B3LYP/6-31G(d) basis set by using the Gaussian 09 program

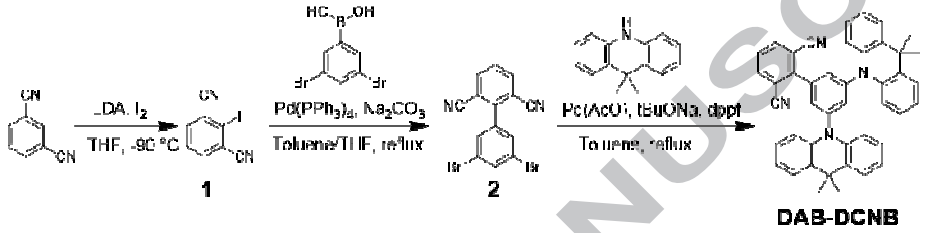

Scheme 1. Synthetic route for **DAB-DCNB**

The thermal properties of the resulting TADF dopant material were measured by differential scanning calorimetry (DSC) and thermogravimetric analysis (TGA), as shown in Figures 2a and 2b, respectively. However, no obvious phase transition process or glass-transition temperature (T_g) was detected for this emitter during the DSC characterization in the 50 to 300 °C range (Table 1). While its decomposition temperature (T_d), which indicates 5% weight loss, is 383 °C (Table 1). These results suggest that this TADF emitter possesses good thermal and morphological stability due to a rigid molecular backbone, and these features are prerequisites for device processing and application.

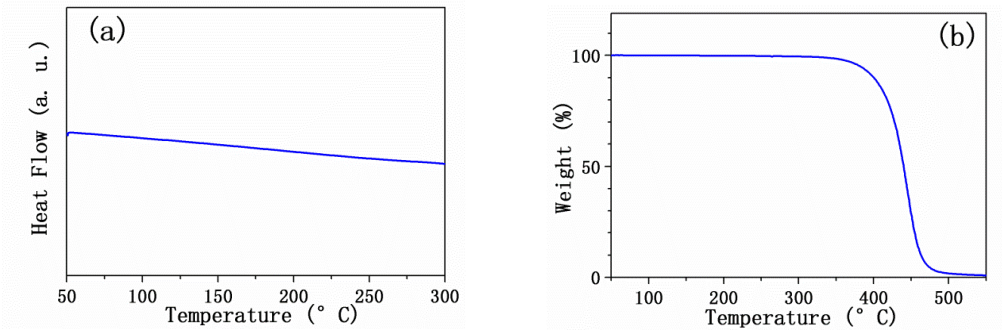

Figure 2. (a) DSC and (b) TGA curves of **DAB-DCNB**

To determine the singlet and triplet energies, the low temperature (77 K) PL spectra of **DAB-DCNB** in toluene were collected, as shown in Figure 3a. According to the fluorescence and phosphorescence emissions, the singlet and triplet energies of

DAB-DCNB were determined to be 3.08 and 3.04 eV, respectively, and therefore, the experimental ΔE_{ST} was determined to be 0.04 eV (Table 1). Such a small ΔE_{ST} and the blue fluorescence emission were due to the *meta*-linkage which not only controls a weak CT state, but also maintains a relatively high triplet energy. The PL and the ultraviolet-visible (UV-Vis) absorption spectra of the studied TADF material in a neat film under ambient condition are shown in Figure 3b. Because of the weak CT interaction between the two 9,9-dimethyl-acridine donors and the dicyanobenzene acceptor, which results from their connections at the *meta*-position, an apparent intramolecular charge transfer band at approximately 350 nm along with a strong n-π^* absorption for the donor moieties at 286 nm were observed in the UV-Vis absorption spectrum (Fig. 3b). The optical band gap of this material was estimated to be 2.86 eV based on the crossing point of the absorption and PL spectra.[26] Due to the rather strong electron-donating capacity of 9, 9-dimethyl-acridine, the neat film of this compound emitted green light with a peak at 508 nm, and the PLQY was 52% (Table 1). However, after blending **DAB-DCNB** into the 1,3-bis (N-carbazolyl)benzene (mCP) matrix with a concentration of 10 w%, the emission peak shifted to 487 nm with an increased PLQY of 61% (Table 1).

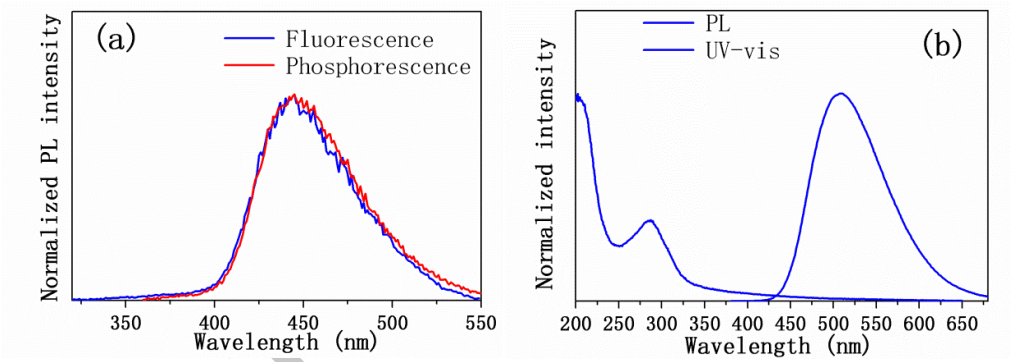

Figure 3. (a) Fluorescence and phosphorescence spectra of **DAB-DCNB** in toluene solution at low temperature (77 K); (b) UV-vis and PL spectra of **DAB-DCNB**'s neat film

The delayed fluorescence behaviors of this compound in the doped film at different temperatures were recorded, and the results are shown in Figure 4. At 300 and 200 K, due to the small ΔE_{ST}, **DAB-DCNB** exhibited a substantial delayed fluorescence component with a lifetime on the microsecond scale. As the temperature decreased to 100 and 10 K, the long lifetime component decreased. This phenomenon indicates that the long lifetime component originated from TADF. The lifetime of the delayed fluorescence at 300 K was 7.1 μs.

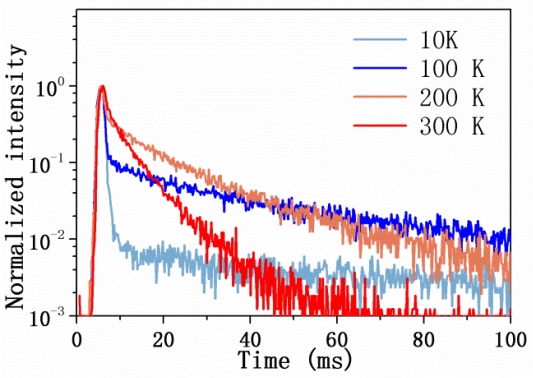

Figure 4. Photoluminescence decays for a thin film of 10 w% DAB-DCNB doped in mCP, measured at temperatures of 10K, 100K, 200K and 300 K

The electrochemical analysis of **DAB-DCNB** was performed. Cyclic voltammetry (CV) was employed to measure the HOMO energy level of this TADF emitter by utilizing ferrocene/ferrocenium (Fc/Fc^+) (with an energy level of 4.8 eV) for calibration. Figure 5 shows the cyclic voltammetry curve, and the onset oxidation potential was 0.27 V. The HOMO energy level of **DAB-DCNB** was calculated to be -5.07 eV (Table 1) according to the following equation (1):

$$\text{HOMO (eV)} = -(E_{ox}^{onset} + 4.8) \quad (1)$$

Therefore, the LUMO energy was estimated to be -2.21 eV (Table 1) by combining the HOMO and optical band gap.

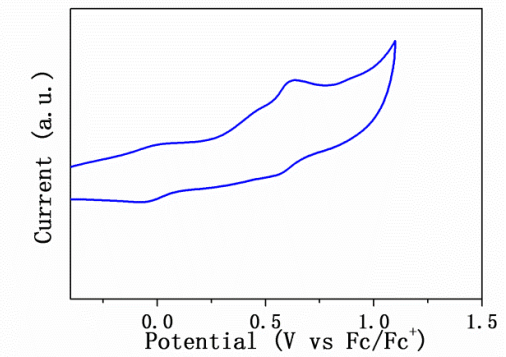

Figure 5. Cyclic voltammograms of **DAB-DCNB**

To assess the electroluminescence properties of **DAB-DCNB**, an OLED device was fabricated by doping the emitter into a mCP host at a concentration of 10% on the basic of photophysical and electrochemical measurement data. The device structure was ITO (120 nm)/ TAPC (25 nm)/ TCTA (5 nm)/ **DAB-DCNB** 10%: mCP (10 nm)/ TmPyPB (50 nm)/ LiF (0.5 nm)/ Al (100 nm) (Fig. 6a), and the molecular structures of the materials used in the OLED device are shown in Figure 6b. In this device, ITO was used as the anode, TAPC (di-[4-(*N*,*N*-ditolyl-amino)-phenyl]cyclohexane) was utilized as the hole-transporting layer (HTL), TCTA (4,4'4"-tri(9-carbazoyl)triphenylamine) was employed as the exciton-blocking layer,

TmPyPB (1,3,5-tri[(3-pyridyl)-phen-3-yl]benzene) was applied as the electron-transporting layer, and LiF/Al was used as the cathode.

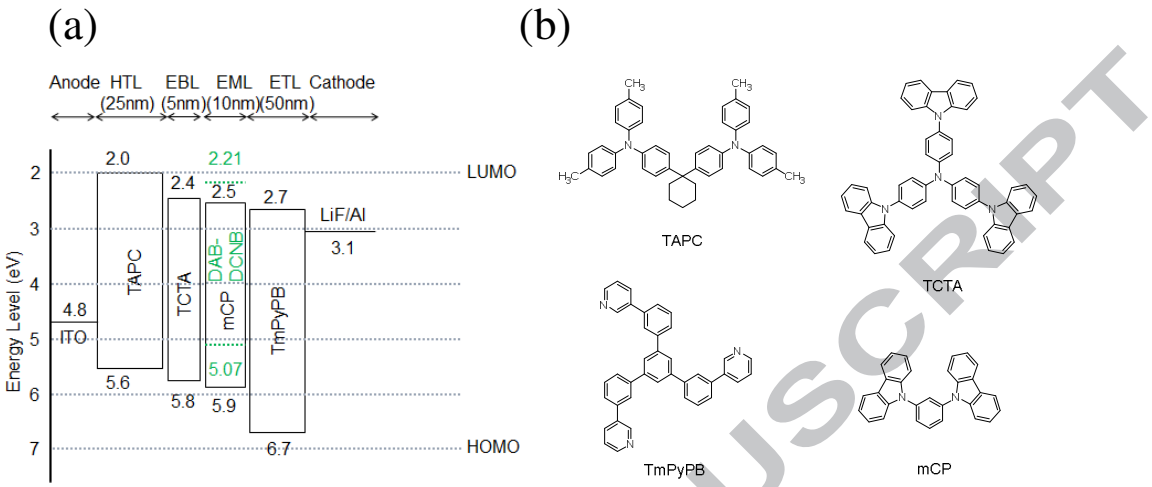

Figure 6. Energy level diagram (a) and molecular structures of the materials used in the OLED device (b)

Figures 7a and b shows the current density (J)-voltage (V)-luminance (L) characteristic of the device as well as the EQE and power efficiency (PE) as a function of the current density (J) curves. In addition, figure 7c shows the current efficiency (CE)-current density (J) characteristic of the device. The OLED device, which employed **DAB-DCNB** as an emitter, turned on at 3.0 V and reached a maximum EQE of 16.5% (Table 2). Considering the limitation of conventional fluorescence devices is only 5-6%, the high EQE is surely due to the contribution of TADF. The maximum current efficiency, power efficiency and maximum luminance were 40.8 cd A^{-1}, 45.8 lm W^{-1} and 5120 cd m^{-2}, respectively (Table 2). As the current increases, the EQE decreased to 10.2%, when the brightness reached 500 cd m^{-2}. This roll-off of efficiency can be ascribed to annihilation of the triplet excitons, and the unipolar characteristic of the mCP host leads to unbalanced charges at a high current density.[27] The key EL performance data for **DAB-DCNB** are summarized in Table 2. The electroluminescence spectrum of the device is shown in Figure 7d. Only the emission that originated from the emitters appeared in the electroluminescence spectrum, which suggested that the charge recombination region was completely confined in the emitting layer. The emission peak of the device was 493 nm (Table 2), which is close to that of the PL spectrum of the emitting layer. The Commission International de l'Eclairage ($CIE_{x, y}$) coordinate was (0.22, 0.38) at 500 cd m^{-2}. In addition, the $CIE_{x, y}$ only varied from (0.22, 0.38) to (0.22, 0.39) over the full operational voltage range (Fig. S7, Supplementary Material). The spectra of the device demonstrated highly stable chromaticity with respect to voltage.

Table 2. EL performance of device based on **DAB-DCNB**

λ_{max} [a] [nm]	L_{max} [cd/m^2]	V_{on} [b] [eV]	CE_{max} [cd/A]	PE_{max} [lm/w]	EQE_{max} [%]	CIE [a] [x,y]
493	5120	3.0	40.8	45.8	16.5	[0.22,0.38]

[a] At current density of 10 mA cm^{-2}.

[b] At luminance of 1 cd m^{-2}.

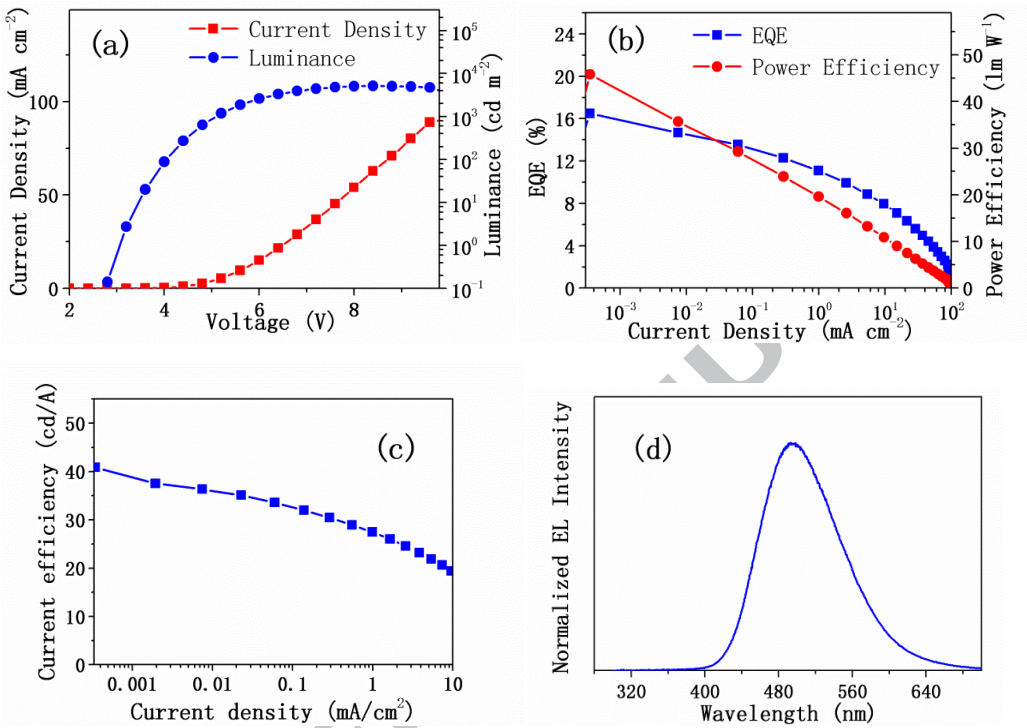

Figure 7. (a) Current density–voltage–luminance curves; (b) EQE and power efficiency versus current density characteristics; (c) Curren efficiency versus current density characteristics and (d) Emission spectrum of the electroluminescence device.

Conclusion

In summary, we have designed and synthesized a novel TADF emitter by connecting a dicyanobenzene acceptor and two 9,9-dimethyl-9,10-dihydroacridine donors at the 1, 3, 5-position of a phenyl ring. This molecule displayed sky-blue emission in a mCP doped film. The *meta*-connected type resulted in a relatively high triplet energy and a small energy difference of 0.04 eV between T_1 and S_1. The novel studied compound was used to manufacture a multilayer electroluminescence device, achieving one of the best performances among devices based on emitters with *meta*-connected types. Due to the TADF features of the emitter, a satisfactory external quantum efficiency up to 16.5% was achieved. We believe that these results may provide a new approach for developing high-performance TADF emitters with *meta*-connected type structures for OLED applications.

Experimental section

Synthesis

2-iodoisophthalonitrile (1): isophthalonitrile (4.48 g, 35 mmol) was dissolved in 200 mL of anhydrous tetrahydrofuran. The solution was cooled to -90 ºC and retained for 0.5 h. Then 28 mL of lithium diisopropylamide (LDA, 1.5 M in tetrahydrofuran, 42 mmol) was added slowly. After the mixture was stirred for 2 h, iodine (12.35 g, 49 mmol) was added. The reaction was retained stirring at -90 ºC for another 2 h and warmed slowly to room temperature. The reaction mixture was poured into water and extracted with dichloromethane. The organic phase was combined and dried over magnesium sulfate. After the solvent was removed, the product was purified by column chromatography on silica gel and then recrystallized in hexane to afford a white solid (4.89 g, 55%). ^{1}H NMR (400 MHz, $CDCl_3$, δ): 7.79 (d, J = 7.6 Hz, 2H), 7.62 (t, J = 8 Hz, 1H). ^{13}C NMR (100 MHz, $CDCl_3$, δ): 137.34, 129.25, 123.44, 118.28, 103.83. MS (APCI, *m/z*): $[M]^+$ calcd for $C_8H_3IN_2$: 254.9; found: 254.8.

2-(3,5-dibromophenyl)isophthalonitrile (2): A mixture of 3,5-dibromophenyl boronic acid (2.51 g, 9 mmol), **1** (2.55 g, 10 mmol), $Pd(PPh_3)_4$ (100 mg) , sodium carbonate (2.12 g, 20 mmol), THF (15 mL), toluene (30 mL), and distilled water (20 mL) was refluxed for 24 h under nitrogen protection. The mixture was extracted with dichloromethane. The organic phases were combined and dried over magnesium sulfate. The crude product was purified by column chromatography on silica gel to afford a white solid (2.57 g, 79%).^{1}H NMR (400 MHz, $CDCl_3$, δ): 7.99 (d, J = 8 Hz, 2H), 7.86 (t, J = 2 Hz, 1H),7.66 (t, J=7.6 Hz, 1H),7.57 (d, J=1.6 Hz, 2H). ^{13}C NMR (100 MHz, $CDCl_3$, δ): 145.67, 137.38, 137.16, 136.06, 130.92, 129.60, 123.66, 115.90, 114.55. MS (APCI, *m/z*): $[M]^+$ calcd for $C_{14}H_6Br_2N_2$: 362.9; found: 362.7.

DAB-DCNB: 9,9-dimethyl-9,10-dihydroacridine (0.92 g, 4.4 mmol) and **2** (0.72 g, 2 mmol) were added into 50 ml toluene. After degassing for 10 min, palladium acetate (22.4mg, 0.1mmol), 1,1'-bis(diphenylphosphino) ferrocene (0.17 g, 0.3 mmol) and sodium *tert*-butoxide (0.58 g, 6 mmol) were added sucessively. Under protection with nitrogen, the mixture was heated to reflux for 24 h with stirring. Then 200 mL of water was added into the reaction mixture and extracted with dichloromethane. The organic phase was combined and dried over magnesium sulfate. After the solvent was removed, the product was purified by column chromatography on silica gel to afford the target compound. The final product was further sublimed at 280 ºC and 4×10^{-3} Pa to give a slight yellow solid (0.75 g, 61%). ^{1}H NMR(400 MHz, $CDCl_3$, δ): 8.00 (d, J = 7.6 Hz, 2H), 7.67-7.63 (m, 3H), 7.57 (t, J =2.0 Hz, 1H), 7.45 (dd, J =1.6, 7.6 Hz, 4H), 7.12-7.08(m, 4H), 6.97(td, J = 1.2, 8.0Hz, 4H), 6.57(dd, J =1.2, 8.0Hz, 4H), 1.66(s, 12H). ^{13}C NMR (100MHz, $CDCl_3$, δ): 147.23, 145.09, 140.49, 139.39, 136.84, 136.02, 132.56, 130.51, 129.43, 126.94, 125.40, 121.34, 116.32, 114.70, 114.38, 36.12, 31.17. MS (APCI, *m/z*): $[M]^+$ calcd for $C_{44}H_{34}N_4$: 619.3; found: 619.2. Anal. calcd for $C_{44}H_{34}N_4$: C 85.41; H 5.54; N 9.05; found: C 85.38, H 5.42, N 9.01.

Acknowledgments

This work has been supported financially by the State Key Laboratory of Fine Chemicals (Panjin) (Grant No. JH2014009) project and the Fundamental Research Funds for the Central Universities.

References and notes

1. Zhang, J.; Li, J.; Chen, W. H.; Zheng, D.; Yu, J. S.; Wang, H.; Xu, B. S. *Tetrahedron Letters*. **2016**, *57*, 2044-2048.

2. Tang, C. W.; VanSlyke, S. A. *Appl. Phys. Lett*. **1987** , *51*, 913-915.

3. Reineke, S.; Lindner, F.; Schwartz, G.; Seidler, N.; Walzer, K.; Lussem, B.; Leo, K. *Nature.* **2009**, *459*, 234-238.

4. Liao, Y.L.; Lin, C.Y.; Wong, K.T.; Hou, T.H.; Hung, W.Y. *Org. Lett*. **2007**, *9*, 4511-4514.

5. Liu, S.J.; He, F.; Wang, H.; Xu, H.; Wang, C.Y.; Li, F.; Ma, Y.G. *J. Mater. Chem*. **2008**, *18*, 4802-4807.

6. Park, Y.; Kim, S.; Lee, J.H.; Jung, D.H.; Wu, C.C.; Park, J. *Org. Electron*. **2010**, *11*, 864-871.

7. Kohler, A.; Wilson, J.S.; Friend, R.H. *Adv. Mater*. **2002**, *14*, 701-707.

8. Yersin, H.; Strasser, J. *Coordin Chem. Rev*. **2000**, *208*, 331-364.

9. Sasabe, H.; Takamatsu, J.; Motoyama, T.; Watanabe, S.; Wagenblast, G.; Langer, N.; Molt, O.; Fuchs, E.; Lennartz, C.; Kido, J. *Adv. Mater*. **2010**, *22*, 5003-5007.

10. Fleetham, T.; Li, G.J.; Wen, L.L.; Li, J. *Adv. Mater*. **2014**, *26*, 7116-7121.

11. Gong, S.L.; Chen, Y.H.; Yang, C.L.; Zhong, C.; Qin, J.G.; Ma, D.G.; *Adv. Mater*. **2010**, *22*, 5370-5373.

12. Goushi, K.; Yoshida, K.; Sato, K.; Adachi, C. *Nat. Photonics.* **2012**, *6*, 253-258.

13. Zhang, Q.S.; Li, J.; Shizu, K.; Huang, S.P.; Hirata, S.; Miyazaki, H.; Adachi, C. *J. Am. Chem. Soc*. **2012**, *134*, 14706-14709.

14. Nakanotani, H.; Higuchi, T.; Furukawa, T.; Masui, K.; Morimoto, K.; Numata, M.; Tanaka, H.; Sagara, Y.; Yasuda, T.; Adachi, C. *Nat. Commun*. **2014**, *5*, 4016.

15. Serevicius, T.; Nakagawa, T.; Kuo, M.C.; Cheng, S.H.; Wong, K.T.; Chang, C.H.; Kwong, R.C.; Xia, S.; Adachi, C. *Phys. Chem. Chem. Phys*. **2013**, *15*, 15850-15855.

16. Endo, A.; Sato, K.; Yoshimura, K.; Kai, T.; Kawada, A.; Miyazaki, H.; Adachi, C. *Appl. Phys. Lett*. **2011**, *98*, 083302.

17. Lee, D.R.; Hwang, S.H.; Jeon, S.K.; Lee, C.W.; Lee, J.Y. *Chem. Commun*. **2015**, *51*, 8105-8107.

18. Hirai, H.; Nakajima, K.; Nakatsuka, S.; Shiren, K.; Ni, J.; Nomura, S.; Ikuta, T.; Hatakeyama, T. *Angew. Chem. Int. Edit*. **2015**, *54*, 13581-13585.

19. Sun, J.W.; Baek, J.Y.; Kim, K.H.; Moon, C.K.; Lee, J.H.; Kwon, S.K.; Kim, Y.H.; Kim, J.J. *Chem. Mater*. **2015**, *27*, 6675-6681.

20. Zhang, D.D.; Cai, M.H.; Zhang, Y.G.; Zhang, D.Q.; Duan, L. *Mater. Horiz*. **2016**, *3*, 145-151.

21. Zhang, Q.S.; Li, B.; Huang, S.P.; Nomura, H.; Tanaka, H.; Adachi, C. *Nat. Photonics.* **2014**, *8*, 326-332.

22. Huang, B.; Yin, Z.H.; Ban, X.X.; Jiang, W.; Dai, Y.; Zhang, J.Y.; Liu, Y.Y.; Yang, Y.P.; Sun, Y.M. *Dyes Pigments.* **2015**, *117*, 141-148.

23. Lee, S.Y.; Yasuda, T.; Park, I.S.; Adachi, C. *Dalton T*. **2015**, *44*, 8356-8359.
24. Huang, B.; Qi, Q.; Jiang, W.; Tang, J.A.; Liu, Y.Y.; Fan, W.J.; Yin, Z.H.; Shi, F.C.; Ban, X.X.; Xu, H.E.; Sun, Y.M. *Dyes Pigments.* **2014**, *111*, 135-144.
25. Usui, S.; Hashimoto, Y.; Morey, J.V.; Wheatley, A.E.H.; Uchiyama, M. *J. Am. Chem. Soc.* **2007**, *129*, 15102-15103.
26. Huang, S.P.; Zhang, Q.S.; Shiota, Y.; Nakagawa, T.; Kuwabara, K.; Yoshizawa, K.; Adachi, C. *J Chem Theory. Comput*. **2013**, *9*, 3872-3877.
27. Masui, K.; Nakanotani, H.; Adachi, C. *Org. Electron*. **2013**, *14*, 2721-2726.

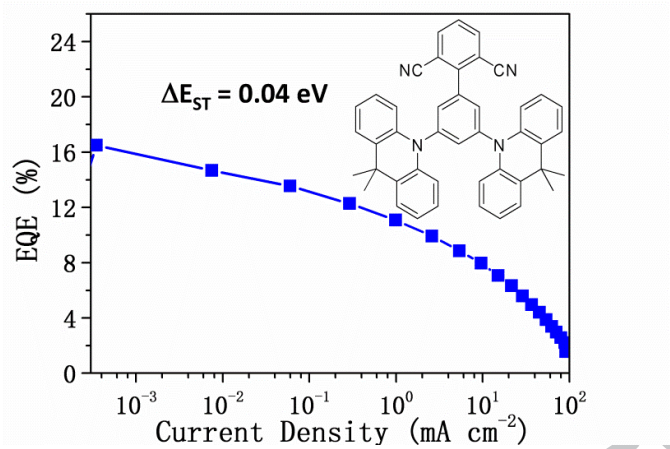

Graphical abstract

1. A dimethylacridines and dicyanobenzene based molecule has been designed and synthesized as a novel TADF emitter.
2. The optical, electrochemical and thermal properties were investigated.
3. The molecule shows a singlet-triplet energy gap as small as 0.04 eV.
4. The doped OLEDs exhibited a high EQE of 16.5%.